AIP Advances

Adsorption of 5-Fluorouracil on Au(111) and Cu(111) surfaces

Cite as: AIP Advances **9**, 085318 (2019); https://doi.org/10.1063/1.5108801
Submitted: 02 May 2019 . Accepted: 08 August 2019 . Published Online: 23 August 2019

Andrew Cassidy, Nataliya Tsud, Sofiia Bercha, Vitaliy Feyer, Kevin C. Prince, and Oksana Plekan

Adsorption of 5-Fluorouracil on Au(111) and Cu(111) surfaces

Cite as: AIP Advances 9, 085318 (2019); doi: 10.1063/1.5108801
Submitted: 2 May 2019 • Accepted: 8 August 2019 •
Published Online: 23 August 2019

Andrew Cassidy,[1] Nataliya Tsud,[2] Sofiia Bercha,[2] Vitaliy Feyer,[3] Kevin C. Prince,[4,5] and Oksana Plekan[4,a)]

AFFILIATIONS

[1]Aarhus University, Department of Physics and Astronomy, Ny Munkegade 120, DK-8000 Aarhus C, Denmark
[2]Charles University, Faculty of Mathematics and Physics, Department of Surface and Plasma Science, V Holešovičkách 2, 18000 Prague 8, Czech Republic
[3]Peter Grünberg Institute (PGI-6) and JARA-FIT, Research Center Jülich, 52425 Jülich, Germany
[4]Sincrotrone Trieste S.C.p.A., in Area Science Park, Strada Statale 14, km 163.5, I-34149 Basovizza, Trieste, Italy
[5]I.O.M.-C.N.R., in Area Science Park, Strada Statale 14, km 163.5, I-34149 Basovizza, Trieste, Italy

[a)]**Corresponding author. Tel.** +39 0403758582; **fax:** +390403758565. **E-mail address:** oksana.plekan@elettra.eu

ABSTRACT

The adsorption of 5-Fluorouracil (5FU) on Au(111) and Cu(111) surfaces as a function of molecular coverage and temperature has been studied, using x-ray photoelectron spectroscopy (XPS) and near-edge x-ray absorption fine structure (NEXAFS) spectroscopy. The nature of 5-Fluorouracil bonding with the two substrates is remarkably different. The Cu substrate forms a chemisorbed complex with 5-FU while the Au substrate shows only physisorption. NEXAFS data at the C, N and O K-edge show a strong angular dependence, indicating that 5-FU lies nearly parallel on the inert Au(111) surface, and at a steep angle on the Cu(111) surface. 5-FU is a biomolecule used for cancer treatment and the results are relevant for those using metal surfaces to prepare 5-FU for applications such as drug delivery.

I. INTRODUCTION

Halogen derivatives of uracil or 5-XU (where X = Cl, Br, F and I, U=Uracil) are important in view of their clinical application.[1–9] As pyrimidine bases, the structural similarity between uracil, or uracil derivatives, and thymine allows for easy *in vivo* incorporation of uracil into DNA.[8] Such modified DNA molecules are susceptible to enhanced radiation damage, which results in increased cell death, an outcome desirable in the case of rapidly multiplying cancer cells.[8] 5-Fluorouracil (5-FU) is often used as a chemotherapy drug[2] and it is an analogue of uracil with a fluorine atom at the C-5 position in place of hydrogen (see Figure 1). The interactions between 5-XU and metallic surfaces and in particular the immobilization of halogenated uracil bases on solid surfaces is, therefore, a key component of many drug-delivery systems.[10–12] Understanding the molecule-substrate interaction is also important for use of these biomolecules in a range different types of applications, including nanotechnology, biosensor engineering, and catalysis.[13–15]

The synthesis of extended molecular architectures, via H-bond intermolecular interactions,[16,17] and the potential for molecular decomposition via intra- or inter-molecular reactions, form the basis of many of the studies examining 5-XU adsorption on metallic substrates.[18–23] Where molecular decomposition dominates, the role of the halogen atom in enabling or preventing scission of the C-X bond has emerged as a key reaction step.[19,24–28] In one of the few experimental surface science investigations targeting 5-FU, Wells *et al.*, have reported that hydrofluoric acid spontaneously forms following a bimolecular reaction between molecules adsorbed on non-pristine metal surfaces, namely Ag.[23,28] In our previous work on 5-XU compounds (X=Br and Cl) and their adsorption on Au(111), we did not observe scission of the C-X bond, but instead observed breaking of the N-H bonds.[29]

Here, we apply x-ray photoelectron spectroscopy (XPS) in combination with near edge x-ray absorption fine structure (NEXAFS) measurements to study the interaction between 5-FU, and Au and Cu substrates. The purpose of the present work is to compare the chemical interactions between 5-FU, and Au and Cu, in an effort

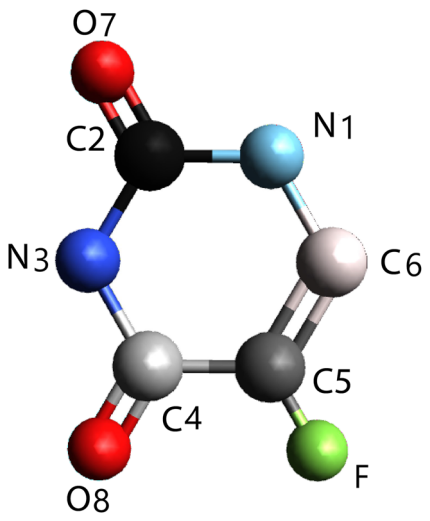

FIG. 1. Molecular structure of 5-Fluorouracil.

to understand any decomposition reactions, and to compare these results to previous work where X=Cl and Br.[29] XPS and NEXAFS are high-resolution spectroscopy techniques that can detect small changes in the average chemical environment experienced by each of the individual atoms in the 5-FU molecule. The Au(111) surface was chosen as an inert substrate[30] to minimize molecule-surface interactions and maximise intermolecular interactions. Cu(111) was chosen as a more catalytically active substrate and has previously been reported to induce decomposition of 5-FU.[28]

II. EXPERIMENTAL

A. Experimental methods

All experiments were performed at the Materials Science Beamline, at the ELETTRA synchrotron light source.[31] The beamline is equipped with a plane mirror monochromator providing synchrotron light in the energy range of 22–1000 eV. The experimental station is equipped with a Specs Phoibos 150 hemispherical electron energy analyzer, low energy electron diffraction (LEED) optics, a dual-anode Mg/Al x-ray source, an ion gun, a gas inlet system, a 5-FU evaporator, and a sample manipulator with a K-type thermocouple attached to the rear side of the sample. The base pressure in the chamber was below 2×10^{-10} mbar.

The Au 4f core level spectra were recorded at a photon energy of 120 eV in normal emission geometry (incidence/emission angles of 60°/0° to the surface normal) and the total resolution (analyser + beamline) was 0.18 eV. The C 1s, N 1s and Au 4f XPS data were collected in the same geometry, and the photon energy and total resolution were 500 eV and 0.50 eV, respectively. The O 1s and F 1s core level spectra were measured at a photon energy of 785 eV with a total energy resolution of 0.85 eV. The Cu 2p core level spectra were taken with the same analyzer using Al Kα radiation as the ionization source, and the total energy resolution was 1.0 eV. All binding energies (BE) were calibrated by measuring the Fermi edge for each photon energy.

The NEXAFS spectra were taken at the C, N and O K-edge using the carbon, nitrogen and oxygen KVV Auger yield (kinetic energy windows 225-275, 355-390, and 495-525 eV, respectively) at two different incident angles, with the electric field almost parallel (GI - 10°) or perpendicular (NI - 90°) to the surface normal. The polarization of light from the beamline has been calculated to be 90% linear, as the source is a bending magnet.[31] The energy resolution in the C, N and O K-edge spectra was estimated to be 0.2, 0.4, and 0.6 eV, respectively. The raw NEXAFS and XPS data were normalized to the intensity of the photon beam, measured by means of a high transmission gold mesh. The data are not normalised to take into account the elemental photo-ionisation cross-sections. In all cases, the corresponding clean Au and Cu surface spectra, recorded under identical conditions, were subtracted.

B. Sample preparation

The samples were gold and copper single crystalline disks of 10 mm diameter and 2 mm thickness with (111) surface orientation purchased from MaTech GmbH. They were cleaned *in situ* using standard procedures: cycles of Ar^+ sputtering (kinetic energy 1.0 keV), followed by annealing at 773-873 K. The surface order and cleanliness were monitored by LEED and XPS. Contaminants (such as C, N, and O) were below the detection limits.

5-FU with the highest commercially available purity was obtained from Sigma-Aldrich and used without further purification. The deposition, using a home-made Knudsen cell type evaporator, was done in a preparation chamber with base pressure of 5×10^{-9} mbar, connected to the analysis chamber. Before deposition, the 5-FU powder was degassed in vacuum at 320 K for several hours, then heated to 340 K and dosed onto the metal surfaces. The coverage of 5-FU was estimated using the parametrized inelastic mean free path for organic materials:[32]

$$\lambda_m = \frac{49}{E_k^2} + 0.11\sqrt{E_K}\ \text{mg/m}^2 \quad (1)$$

where *Ek* is the kinetic energy of photoelectrons. The λ_m value was converted to distance by dividing by the density of 5-FU powder ($1.5\text{x}10^9$ mg/m^3).[33] The inelastic mean free path for Cu $2p_{3/2}$ (excited by 1486.6 eV photons) and Au $4f_{7/2}$ (excited by 500 eV) photoelectrons passing through the 5-FU adlayer was equal to 1.73 nm and 1.5 nm, respectively. Using these values, the effective thickness of adsorbed molecules on the surface was calculated using the equation:

$$I_d = I_0 e^{\left(-\frac{d}{\lambda_m}\right)} \quad (2)$$

where I_d and I_0 are the attenuated and clean surface intensity of the photoelectron signal and d is the thickness of the molecular adlayer. After 5 min and 10 min deposition of 5-FU on either substrate the film thickness remained the same 3.2 Å ± 5%, indicating formation of a thin layer without further adsorption. We refer to monolayer (ML) films below, prepared by annealing a saturated coverage to 350 K or 450 K for Au(111) and Cu(111) respectively. The annealing step was included in order to desorb any weakly adsorbed 5-FU species not directly related to the metal-monolayer interface.

Organic molecules have a tendency to dissociate when exposed to ionizing radiation. Valence band (VB) photoemission spectra of the saturated layer and ML films of 5-FU were measured at 120 eV photon energy to check for radiation damage. The beamline has a

high photon flux at 120 eV and the cross-section for absorption is high. No spectral changes were observed after 1 hour of exposure to radiation and we conclude that our molecular films were stable under these experimental conditions.

III. RESULTS AND DISCUSSION

A. Core level spectra

The experimental C 1s, N 1s, O 1s and F 1s photoemission spectra of saturated (as-deposited) and monolayer (1 ML) films of 5-FU on Au(111) and Cu(111) substrates are presented in Figures 2 and 3, respectively. The energies of the observed spectral features and proposed assignments are listed in Tables I and II. For comparison, binding energies of 5-BrU and 5-ClU monolayer films, produced by evaporation onto Au(111), are also listed in Table I.[29] A quantitative analysis of the XPS data was performed in order to check the atomic stoichiometry of the molecular film. 5-FU is composed of C, N, O and F atoms in the ratio 4:2:2:1 and we found that the experimental stoichiometry (relative to F≡1) inferred from the fitted XPS spectra measured with Al Kα radiation is C:N:O:F=4.3:2.1:2:1, which is close to the expected values. For peak fitting, a Shirley background was subtracted and the data were fitted with Voigt functions, one for each ionic state.

1. 5-FU on Au(111)

The majority of the C 1s core level spectrum of 5-FU on Au(111), Fig. 2(a), can be deconvoluted into 4 peaks, one for each C atom in the molecule,[23,29] see Table I. This assignment is in agreement with gas-phase data[34] and previous XPS data for uracil adsorbed on different metal surfaces.[17,25,35–38] We note, that the C5 and C6 atoms have very similar binding energies and from the data alone it is not possible to distinguish between the binding energies for these atoms. After annealing, the position of the peak attributed to the C5 and C6 atoms (286.24 eV) (see Fig. 2(a)) is close to the recently published data for 4-Fluorothiophenol monolayer adsorbed on Ni(111).[39] F. Blobner *et al.* have attributed the component at 286.5 eV to a carbon atom bounds to the highly electronegative fluorine substituent.[39] There is a small amount of intensity at lower

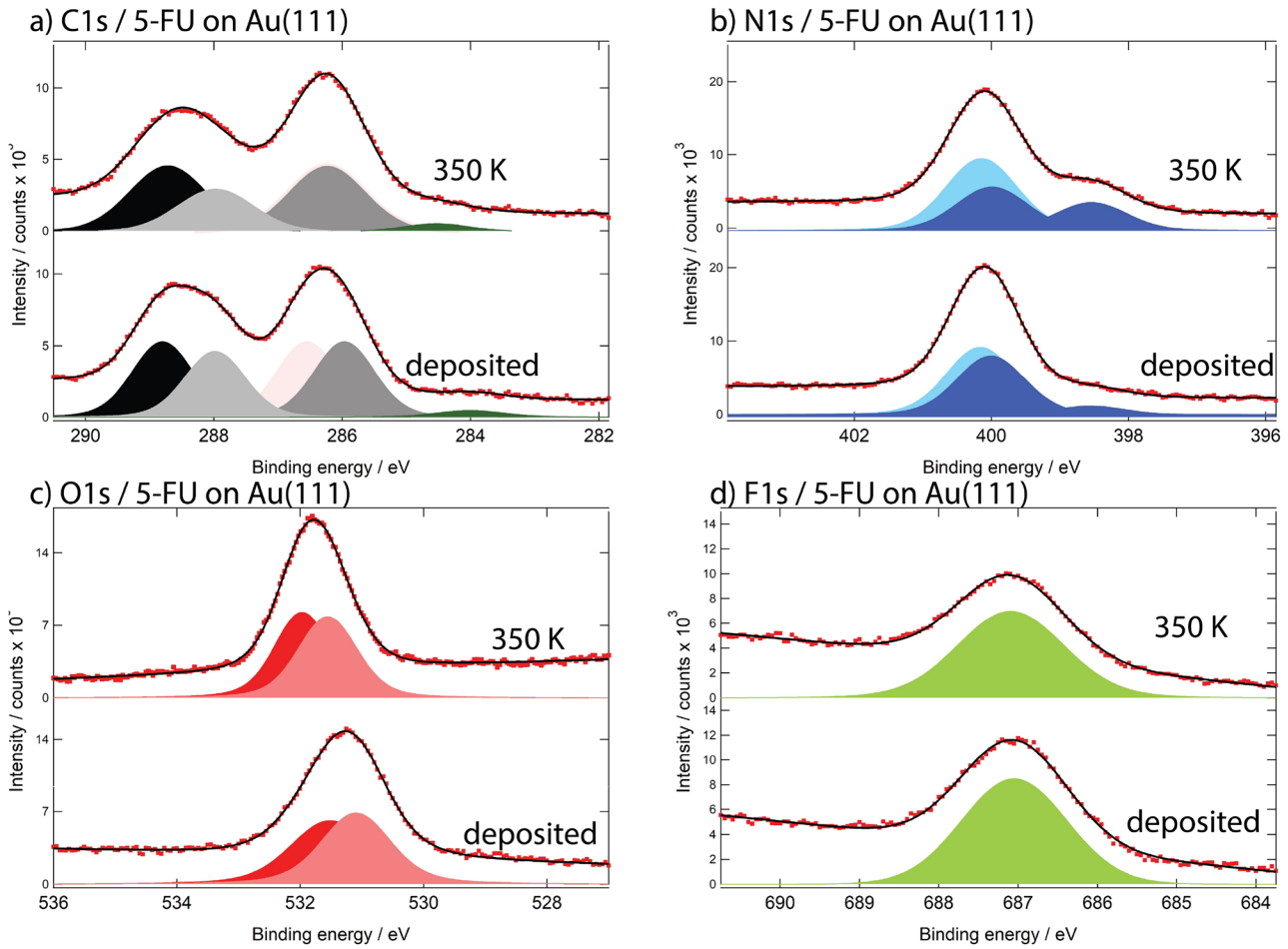

FIG. 2. 5-Fluorouracil XPS spectra of (a) C 1s, (b) N 1s, (c) O 1s, and (d) F 1s core levels corresponding to the deposited layer and after annealing to 350 K on Au (111). The raw data appear as red squares with the fits as black lines. The fit components are shown with subtracted background.

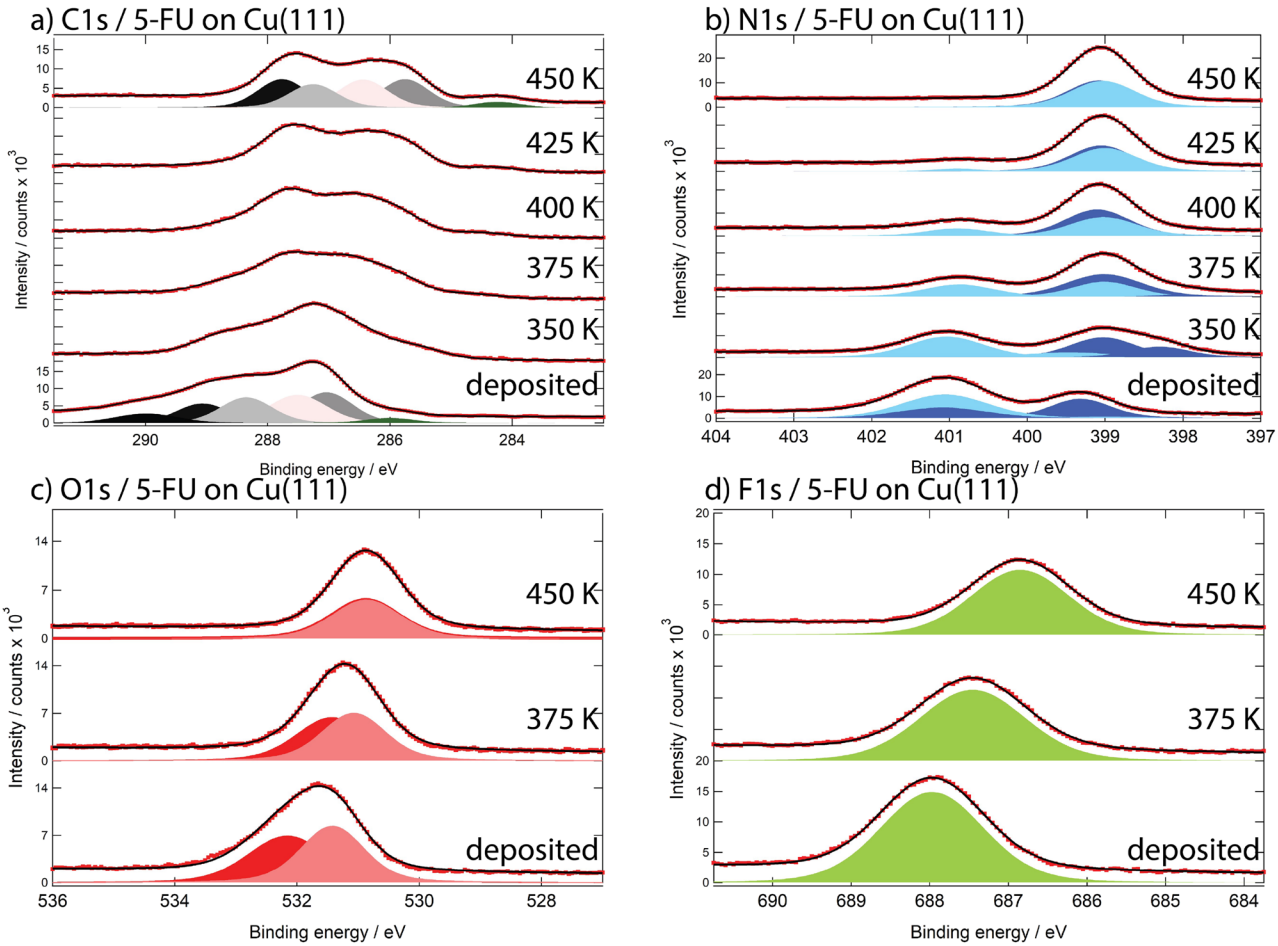

FIG. 3. 5-Fluorouracil XPS spectra of (a) C 1s, (b) N 1s, (c) O 1s, and (d) F 1s core levels of the coverage when deposited on Cu(111), and as a function of annealing temperature. Red squares represent the raw data and black lines result from the fits. The fit components are shown with subtracted background.

TABLE I. C, N, O and F 1s binding energies of 5-FU adsorbed on Au(111).

	5-FU, Deposited	5-FU, 350K	5-BrU on Au(111), 1ML,[29]	5-ClU on Au(111) (multilayer/1ML[29]
C 1s	288.80 (C2)	288.72 (C2)	288.77	288.45/288.63
	288.00 (C4)	288.00 (C4)	287.87	
	286.55 (C6)	286.24 (C6)	285.62	/287.73
	285.97 (C5)	286.24 (C5)	285.12	285.65/285.38
	284.00 (C-, F-loss)	284.55 (C-, F-loss)		
N 1s	400.1 (N1)	400.1 (N1)	399.92	400.1/399.91
	400.0 (N3)	400.0 (N3)		
	398.5 (N3)	398.5 (N3)		
O 1s	531.0	531.1	531.75	531.85/531.70
	531.5	531.7		
F 1s	687.0	687.1		

TABLE II. C, N, O and F 1s binding energies of 5-FU adsorbed on Cu(111).

	C 1s	N 1s	O 1s	F 1s
5-FU, Deposited	289.99 (C2) 289.07 (C2) 288.35 (C4) 287.51 (C6) 287.04 (C5) 286.00 (C-, F loss)	401.1 (N1) 401.1 (N3) 399.3 (N3[a])	532.2 531.5	688.0
After annealing to: 350K	288.48 (C2) 288.06 (C2) 287.80 (C4) 287.25 (C6) 286.60 (C5)	401.0 (N1) 399.5 (N1[a]) 399.0 (N3[a]) 398.3 (N3[a])		
375K	288.70 (C2) 287.80 (C2) 287.40 (C4) 286.70 (C6) 285.97 (C5)	400.9 (N1) 399.0 (N1[a]) 399.0 (N3[a])	531.4 531.2	687.5
400K	288.70 (C2) 287.82 (C2) 287.42 (C4) 286.64 (C6) 285.93 (C5)	400.9 (N1) 399.0 (N1[a]) 399.1 (N3[a])		
425K	288.70 (C2) 287.77 (C2) 287.30 (C4) 286.49 (C6) 285.78 (C5)	400.9 (N1) 399.0 (N1[a]) 399.1 (N3[a])		
450K	287.77 (C2) 287.26 (C4) 286.44 (C6) 285.75 (C5) 284.24 (C-, F loss)	399.00 (N1[a]) 399.00 (N3[a])	530.9 530.8	686.8

[a]indicates the binding energy for a deprotonated N atom.

binding energy, 284.0 eV, and we attribute this to a small fraction of molecules that have lost the F atom upon deposition. The binding energy of 284.0 eV fits with C5 atoms in 5-HU indicating that the deposition process did lead to a very small degree of decomposition. However, the amount of C described by this peak did not change when the film was annealed to 350 K, indicating that no further decomposition occurred. Our assignment in Table I is based on an analysis of literature values for uracil[17] and 5-HU.[29]

The N 1s core level spectrum of 5-FU deposited on the Au(111) surface is presented in Fig. 2(b). On deposition, a single peak with a weak low energy shoulder is observed, indicating N1 and N3 have almost identical BE after deposition.[23,28,29] After annealing, a clear peak emerges at the location of the shoulder, and has a binding energy of 398.5 eV; this is accompanied by a very slight shift of the main peak. Binding energies around 400.0 eV are attributed to intact 5-FU species weakly bonded to the Au substrate via van der Waals interactions and the BE is identical to that reported for bulk-like 5-FU by Mazzola *et al.*[23] Mazzola *et al* and Peeling *et al.* have attributed low BE N 1s photoelectrons to dehydrogenated N atoms.[23,25] We found the difference in binding energy between the two peaks used to describe the N3 atoms in Fig. 2b as 1.4 eV, and this number is in good agreement with values observed for anionic uracil[25] as well as with the density functional theory data for the pyrimidine nucleobase.[26,27] We assign the high binding energy peaks around 400 eV to neutral amino nitrogen atoms N1 and N3, and the peak at 398.5 eV to an anionic form of a deprotonated N atom. The fraction of deprotonated N is not stoichiometric, indicating that only a small fraction of 5-FU lose a H atom and the majority remains intact on the Au(111) substrate. While the data do not allow us to distinguish between deprotonation at the N1 and N3 sites, we propose

that deprotonation occurs at the N3 position, as this site appears to be the more acidic in other studies.[40] Risinggård *et al* interpreted the appearance of a deprotonated N3 atoms as evidence of a chemical reaction between the 5-FU thin-film and a Ag substrate.[28] No such reaction was reported between 5-BrU or 5-ClU and Au when species were deposited from the gas phase.[29]

The oxygen and fluorine photoemission data of 5-FU are shown in Fig. 2(c, d). The peaks in the O 1s data are assigned to the carbonyl oxygen atoms O7 and O8.[34] While two peaks were used to fit the O 1s intensity we cannot distinguish between O7 and O8. The similar BEs imply that both oxygen atoms inhabit similar chemical environments and the slight shift after annealing may result from charge transfer. The F 1s spectra can be fitted with a single broad peak centred at 687 eV and this value is a good match to that reported for 4-Fluorothiophenol on Ni(111) by F. Blobner *et al.*[39] We note there that there is no change in ratio between the intensity of electrons arising from the O 1s state and electrons from the F 1s state after annealing, within a 5% error. This implies that the ratio between F and O remains stoichiometric, according to that expected from the molecular structure. Mazzola *et al.* reported a reduction in the F/O ratio, indicating F loss when 5-FU is annealed on Ag but we found no evidence for F desorption from the molecule on the Au substrate after the small, initial F-loss following deposition. Qualitative comparison between the data here, describing 5-FU adsorbed on Au(111), and data collected by Mazzola *et al.*,[23] which describe bulk films of 5-FU, reveal some slight shifts in all peak positions to lower binding energies that we can attribute to interactions between the molecule and the Au substrate. There is no deprotonation at the N3 position reported for the bulk films and, accordingly, no N 1s intensity was reported for binding energies below 400 eV.

2. 5-FU on Cu(111)

The core level spectra for C 1s, N 1s, O 1s, and F 1s of 5–FU on Cu(111) as a function of annealing temperature are presented in Figure 3 and the energies of the peaks and assignments are summarized in Table II. In contrast to 5-FU on Au, the spectra of molecules adsorbed on Cu continued to evolve as the annealing temperature was raised, and so data up to 450 K, the onset for molecular desorption, are reported.

The range of BEs for C 1s peaks immediately following deposition is broader than has been reported for 5-FU molecules on Au, Fig. 2a, or for bulk-like 5-FU,[28] indicating a role for the Cu substrate. The low binding energy peak attributed to molecules that loose the F-atom during deposition in Figure 2a also appears here, again at low binding energy. As with Au(111), the intensity of this peak did not increase as the sample was annealed further suggesting no further decomposition and we relate the loss of F to the sample deposition process. Throughout the fitting process, it was assumed that the stoichiometric relationship between the 4 carbon atoms in the molecule remained intact, with only the C2 atom borrowing intensity from multiple peaks in order to fit the data. Upon deposition, the intensity of electrons from the C2 atom is split into 2 peaks, with high binding energies and as the sample is annealed to 450 K these two peaks merge into one. It was again difficult to distinguish between the binding energies at the C5 and C6 positions using the data alone. We note that after annealing to 350K, the position of the peak attributed to the C5 atom (carbon bound to the highly electronegative fluorine) moves close to that published by F. Blobner *et al.*[39] All peaks shift to a lower binding energy as the annealing temperature is increased. This indicates a change in the chemical environment for all C atoms. See Table II for peak assignment details. The assignment of the low binding energy peaks observed in C 1s spectra after annealing to 450 K fits with that proposed for doubly deprotonated uracil on Cu(111).[17] We propose that the shift to low binding energy observed for all peaks as the annealing temperature increases arises from deprotonation of the molecule; first a deprotonation at one N atom and finally deprotonation at both. All assignments in Table II are based on literature values for uracil[17] and 5-HU.[29]

The N 1s core level spectra of 5-FU deposited on the Cu(111) surface exhibit dramatic changes as the annealing temperature is increased (see Fig. 3(b)). Two well resolved peaks in the spectra are visible immediately after deposition and these become one peak as the annealing temperature is increased. We propose that these two peaks represent two distinct chemical environments for N atoms in the 5-FU molecule; high binding energy signifies intact N-H bonds, while low binding energies signify deprotonated N atoms. The non-stoichiometric ratio between the two peaks indicates that each N atom on the molecule can be found in both of these states upon deposition, i.e., some N atoms are deprotonated but not all, but by 450 K both N atoms are deprotonated. This is in good agreement with published data for uracil molecules on Cu(111) and Cu(110) surfaces[17,40] and thymine on TiO_2.[41] The analysis in these refs leads us to conclude that the N3 atom is likely to deprotonate first, followed by the N1 atom. The suggestion that only partial deprotonation has occurred at the N3 position following deposition concurs with the splitting of the intensity for the C2 carbon peak in Figure 3a. That is, we propose that a deprotonation at N3 position results in a shift to lower binding energies for the C2 peak. At 350 K a new shoulder at low binding energy begins to emerge but disappears again at 375 K. This shoulder may represent a transient, stronger interaction between a deprotonated N atom and the Cu substrate at 375 K, but there are no reports of such a low binding energy peak in other spectra for 5-XU species.

As with 5-FU on Au, the O 1s spectra for 5-FU on Cu can be fit with two broad peaks, one for each of the O atoms in the molecule. The observed shift in the peak energies following annealing is identical to that reported for uracil adsorbed on Cu(111) and Cu(110) surfaces,[17,40] and concurs with the proposal that the molecule deprotonates as the temperature increases. The F 1s core level appears as a single feature at binding energy of 688.0 eV upon deposition and the binding energy decreases to 686.8eV at 450 K which is similar to that observed for 4-Fluorothiophenol on Ni(111) by F. Blobner *et al.*[39] We attribute this shift to electron redistribution in the molecule following the double deprotonation.

As for 5-FU on Au, there was no change in ratio between the intensity of electrons arising from the O 1s state and electrons from the F 1s state after annealing, within a 5% error. This implies that the ratio between F and O remains stoichiometric, as expected from the molecular structure, and again there is no evidence for F desorption from the molecule.

The adsorption behavior of 5-FU on Cu is different to that on Au. The increase of the deprotonated N signal as a function of annealing 5-FU on Cu indicates a strong interaction with the substrate. The non-stoichiometric ratio of features observed for N 1s spectra of 5-FU on Cu confirms that there are at least two

chemically distinct molecular adsorption states present. The high BE peak in the N 1s spectra corresponds to the two nitrogen atoms (N1, N3 amino) weakly bonded with Cu(111) substrate, while the lower BE peak is related to the nitrogen atom (N3 imino) deprotonated upon adsorption. The deposition of 5-FU in vacuum at room temperature induces some deprotonation and annealing completes this reaction.

B. NEXAFS and molecular orientation

Polarization-dependent NEXAFS is an efficient tool to obtain information on the conformation and orientation of adsorbed molecules. NEXAFS features are more intense when the dipole direction of the excitation in the molecule lies parallel to the plane of polarisation in the incoming photon. Therefore, by adjusting the photon incidence angle, θ; the angle between the linear polarization of the light and the surface normal, we can learn about the orientation of a molecule on the substrate surface.[42] The C, N and O K-edge NEXAFS spectra, measured at normal and grazing incidence of the photon beam with respect to the surface for films of 5-FU deposited onto Au(111) and Cu(111) surfaces are presented in Figures 4 and 5. The peak positions and assignments are summarized in Tables III and IV.

1. NEXAFS spectra of 5-FU on Au(111)

The experimental C, N and O K-edge NEXAFS data deposited films of 5-FU on Au(111) measured at grazing incidence (GI) and normal incidence (NI) geometries are shown in Fig. 4. For aromatic systems such as 5-FU, the π^* states are derived from p_z orbitals oriented perpendicular to the molecular plane. If the aromatic π^* system lies parallel to the surface, the intensity of the corresponding transitions in the spectra is maximised at GI and vanishes at NI.[42] In the data presented here, C, N and O K-edge NEXAFS spectra have been divided into two ranges: lower photon energy and higher photon energy. The well-resolved, intense peaks in the low-photon-energy range for all K-edges were assigned to transitions involving π^* orbitals, while broad, less-intense features in the high-photon-energy range are assigned to σ^* orbitals. The corresponding assignments for all transitions (see Table III) were based on available gas phase data for uracil[34] and experimental NEXAFS data for condensed 5-halouracils prepared on Ag/Au surfaces[23,28,29] and uracil adsorbed on Au(110) and Ag(111) metal substrates.[36,17]

The C K-edge NEXAFS data (see Fig. 4(a)) are dominated by four main bands arising from resonances associated with the four carbon atoms of the pyrimidine ring. Our experimental C K-edge NEXAFS data for 5-FU on Au(111) surface are in good agreement with the data published for uracil adsorbed on Au(110) and Ag(111), see Table III. The first peak at 284.8 eV is attributed to the C5→$\pi^*_{C=C}$ transition, while the second peak at 285.8 eV is due to the same transition but from the C6 carbon atom. The next pair of resonances, at 288.4 eV and 290.6 eV, result from the C4 1s → $\pi^*_{C=O}$ and C2 1s → $\pi^*_{C=O}$ transitions respectively. The broad features at higher photon energy are assigned to C 1s→σ^* transitions. The stronger intensity of the π^*peaks at GI geometry and the partial disappearance of these peaks, relative to the σ^* peaks, at NI indicates that the pyrimidine ring of 5-FU is oriented parallel to the Au (111) surface.

N K-edge NEXAFS spectra of 5-FU measured at GI incidence show six maxima, see Fig. 4(b). On the basis of x-ray absorption spectra for 5-BrU and 5-ClU condensed on a Au(111) substrate,[29] the first three features at low photon energy have been assigned to the excitation of N1 and N3 1s core electrons to the LUMO ($\pi^*_{N-C\ amide}$) and LUMO+1 ($\pi^*_{N-C\ amide}$) respectively. The other

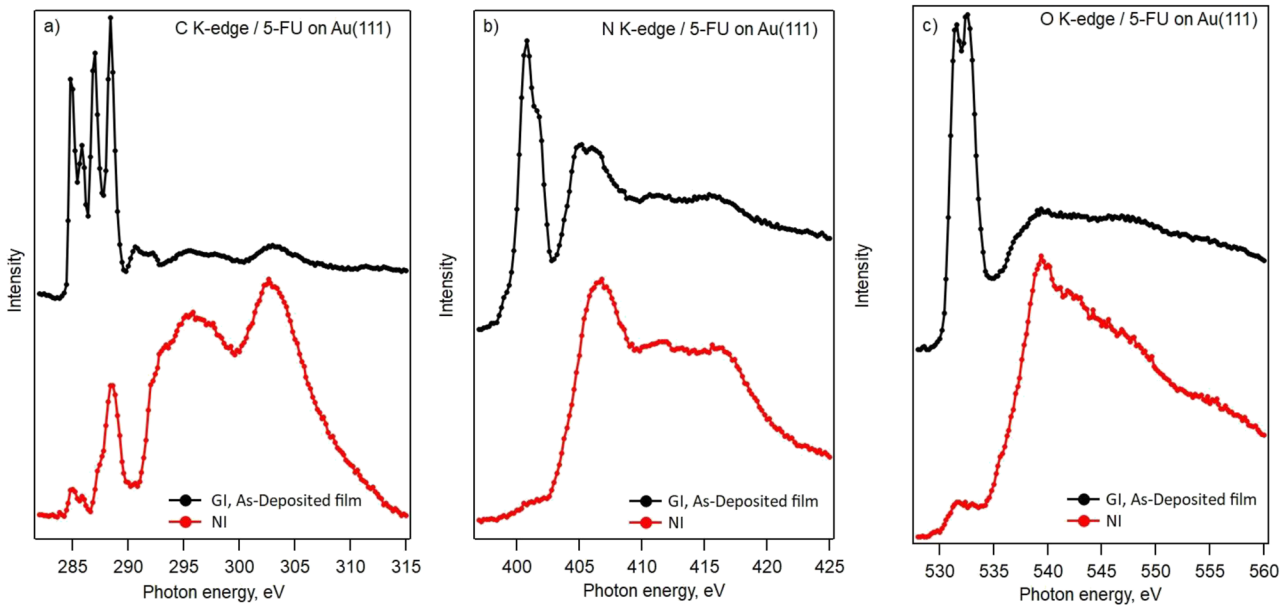

FIG. 4. C (a), N (b) and O (c) 1s NEXAFS spectra of 5-Fluorouracil adsorbed onto Au(111) measured at GI and NI incidence.

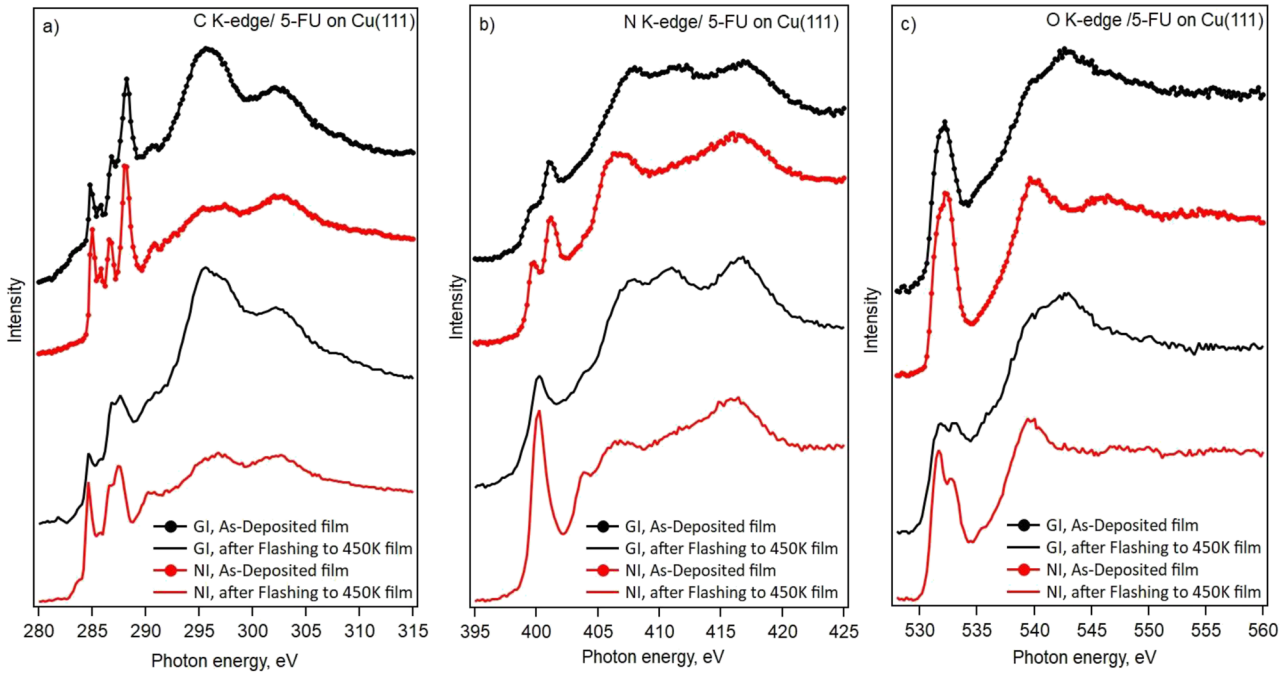

FIG. 5. C (a), N (b) and O (c) K edge NEXAFS spectra of 5-Fluorouracil adsorbed on Cu(111), measured at GI and NI incidence for two different film thicknesses.

three broad peaks lying at higher photon energy range were assigned to N 1s→$\sigma^*_{(N\text{-}C=O)}$ transitions. The O K-edge spectra of 5-FU shown in Fig. 4(c) have also been divided into π^* and σ^* regions. The two intense peaks at 531.6 and 532.6 eV were assigned to the transitions O7 1s→π^* and O8 1s→π^*, respectively. The broad feature at 539.6 is due to the excitation to σ^* resonances of the two oxygen atoms in this molecule.[34] Both experimental N and O K edge NEXAFS data for 5-FU demonstrate strong angular dependence: the π^* resonances

TABLE III. Position and assignment of the individual peaks in the C, N and O 1s NEXAFS spectra of 5-Fluorouracil adsorbed onto Au(111).

K-Edge	GI, eV	NI, eV	Uracil on Au(110)[36]	Uracil on Ag(111)[17]	5-BrU on Au(111)[29]	5-ClU on Au(111)[29]
C 1s	284.8 (π^*)	284.8 (π^*)	284.8	284.7		
	285.8 (π^*)	285.8 ($\pi*$)	286.0	285.9		
	287.0 (π^*)	287.0 (π^*)	287.0	286.4		
	288.4 (π^*)	288.4(π^*)	288.2	288.0		
	290.6 (π^*)	290.6(π^*)	289.6	289.4		
	292.2 (π^*)	292.2 (π^*) (shoulder)	291.6	290.2		
				293.5		
	295.8 (σ^*)	295.8(σ^*)	296.0	295.0		
	303.0 (σ^*)	303.0(σ^*)	303.6	303.0		
N 1s	400.8 (π^*)		400.9		400.9	401.0
	401.8 (π^*)	401.8 (π^*) (shoulder)	401.9		401.7	402.0
	405.0 (π^*)		404.7		404.7	405.0
	406.6 (σ^*)	406.6(σ^*)			406.3	406.8
	411.2 (σ^*)	411.2(σ^*)				
	415.8 (σ^*)	415.8(σ^*)	416.3		415.5	415.4
O 1s	531.6(π^*)	531.6(π^*)	532.3		531.4	531.55
	532.6(π^*)				532.6	532.95
	539.6(σ^*)	539.6(σ^*)	540.7		540.2	540.15
			547.7		546.0	548.15

TABLE IV. Energies and assignments of the peaks in the C, N and O K NEXAFS spectra of 5-Fluorouracil adsorbed on Cu(111).

K-Edge	GI, eV	NI, eV	GI, flash to 450K	NI, flash to 450K	Uracil on Cu(111)[17] Cu(110)[40,44,45]
C 1s	284.8(π^*)	284.8(π^*)	284.6(π^*)	284.6(π^*)	284.9
	285.8(π^*)	285.8(π^*)	285.6(π^*)	285.6(π^*)	286.0
	286.8(π^*)	286.8(π^*)	286.8(π^*)	286.8(π^*)	286.4
	288.2(π^*)	288.2(π^*)	287.6(π^*)	287.6(π^*)	287.9
	290.6(π^*)	290.6(π^*)	290.6(π^*)	290.6(π^*)	289.2, 292.1
	295.8(σ^*)	295.8(σ^*)	295.8(σ^*)	295.8(σ^*)	295.0
	302.6(σ^*)	302.6(σ^*)	302.6(σ^*)	302.6(σ^*)	302.0
N 1s	399.8(π^*)	399.8(π^*)	400.2(π^*)	400.2(π^*)	398-404
	401.2(π^*)	401.2(π^*)	403.8(π^*)	403.8(π^*)	
	407.8(σ^*)	406.6(σ^*)	407.8(σ^*)	406.6(σ^*)	408
	411.0(σ^*)		411.0(σ^*)		
	416.8(σ^*)	416.8(σ^*)	416.8(σ^*)	416.8(σ^*)	415
O 1s	532.2(π^*)	532.2(π^*)	531.6(π^*)	531.6(π^*)	531-534
			533.0(π^*)	533.0(π^*)	
	539.6(σ^*)	539.6(σ^*)	539.8(σ^*)	539.8(σ^*)	
	542.6(σ^*)		542.6(σ^*)		538-543

are stronger than the σ^* resonances at GI geometry, while at NI the intensity ratios reverse, and the π^* resonances disappear almost completely. This provides further proof that the 5-FU molecules are oriented parallel to the Au(111) surface. The results of the N 1s and O 1s NEXAFS spectra are consistent with data published by Fujii and co-authors.[43] They found that uracil and its halogenated forms are orientated and tilted at a small angle with respect to a Au-coated Si surface, although other pyrimidines such as thymine and cytosine were randomly oriented.[43]

2. NEXAFS spectra of 5-FU on Cu(111)

The C, N and O K-edge NEXAFS spectra recorded at GI and NI angles with respect to the Cu(111) surface, for deposited and annealed MLs of 5-FU are shown in Fig. 5. The assignment of the peaks was made on the basis of data published for pyrimidine based molecules condensed on Cu(111) and Cu(110) surfaces[17,40,44,45] (see Table IV). As with the XPS data presented in Figure 3, NEXAFS spectra of 5-FU on Cu(111) exhibit changes after annealing to 450 K.

Linear dichroic effects at the C K edge NEXAFS spectra for 5-FU are more pronounced for Au(111) than for Cu(111). On Cu(111), the σ^* resonances are stronger than the π^* resonances at GI and vice versa at NI. This indicates that molecules do not lie parallel to the substrate, as was the case for 5-FU on Au(111). Annealing to 450 K leads to a small difference in dichroism and the position of peaks is slightly shifted. The peak shifts correlate with deprotonation at the two N atoms, as described in Figure 3. σ^* resonances are stronger again after the anneal to 450 K.

NEXAFS spectra for the N K-edge show little angular dependence, with π^* resonances appearing less intense than σ^* resonances in both GI and NI, Fig. 4(b). Four features can be identified in the NEXAFS spectra of multilayers of 5-FU, recorded after deposition; two π^* resonances and two σ^* resonances. The N 1s XPS data in Fig. 3(b), hinted that at least one of the N atoms is deprotonated immediately upon film growth and here, the first peak at 399.6 eV, is related to the transition between a deprotonated N3 atom and the unoccupied π^* orbital. The second peak at 401.2 eV is ascribed to the protonated N1 1s→π^* resonance transition. The broad features observed in the N K-edge NEXAFS spectra at high photon energy, in the range between 406-417 eV, for both geometries are attributed to N1, N3 1s→ σ^* (N-C) shape resonances.

After annealing to 450 K only a single peak remains in π^* resonances at 400.2 eV, and it is assigned to the deprotonated N3/N1 1s→π^* resonance transition. This behavior matches well with the observation of the single peak at 399.0 eV in the N 1s XPS spectra of 5-FU on Cu(111) after annealing to 450 K. The dichroism after annealing is slightly more pronounced, as with the C K-edge, again suggesting that the molecule adopts a more upright configuration.

The O K-edge NEXAFS spectra of 5-FU adsorbed on Cu(111) can be divided into two regions; features at the absorption edge from 531-534 eV, and broader features at higher energy range from 538-540 eV. The doublet feature between 530 eV and 535 eV is more clearly resolved after annealing to 450 K and it is assigned to O7, O8 1s→π^* transitions, while the broad peaks at higher energies are assigned to the excitation of σ^* resonances of the two oxygen atoms.

The dipole moment of the 1s→π^* transition is oriented perpendicular to the pyrimidine ring, and so the vanishing intensity of the π^* resonances at NI indicates that 5-FU lies parallel to the Au(111) surface. On the contrary, on Cu(111) at GI, the σ^* resonances are stronger than the π^* resonances and vice versa at NI. The angular dependence of the π^* resonance intensity varies as $I \propto \cos^2\theta$,[42] where θ is the angle between the E-vector and the orbital dipole moment. Using this equation, we find that the 5-FU adsorbs on Cu(111) with a tilt angle of 58°±5° from the surface plane, and this increases to 63°±5° after annealing to 450 K. This is in keeping with previous reports describing the adsorption of uracil on Cu surfaces.[17]

We note that the deprotonation of the 5-FU molecule that results from heating on the Cu(111) substrate leads to only a small change in the angle at which the molecule sits on the surface. This indicates that following deposition, and the initial partial deprotonation at the N3 position, the molecule adsorbs in a stable geometry. It is likely that this configuration sees both O atoms in direct contact with the Cu surface. Indeed, DFT calculations have suggested this configuration for the adsorption of 5-HU on Cu(111).[17] This suggested geometry does not allow for the second N atom in the N1 position to approach the Cu substrate. That this stable geometry does not change significantly when a second deprotonation occurs at the N1 position therefore hints that it is the Cu-O interaction that initiates the deprotonation mechanism.

IV. CONCLUSIONS

The combination of XPS and NEXAFS spectra has provided a clear picture of 5-FU adsorption behavior on the Au and Cu substrates.

On the basis of XPS data, we conclude that the 5-FU deposited on Au(111) weakly adsorbs on the metal substrate and an annealing to 350 K only causes a slight degree of deprotonation, most likely at the N3 component. In contrast, the spectra of 5-FU films formed on the more reactive Cu(111) show the presence of a strongly adsorbed molecule. The stronger interaction leads to deprotonation at the nitrogen atoms and the formation of this chemical state is complete following annealing to 450 K. In addition, all C, N and O NEXAFS spectra of the 5-FU show strong angular dependence, indicating local ordering. For 5-FU on Au, the π^* absorption features are reduced at normal incidence (NI) relative to the measurement at grazing incidence (GI) angles, indicating that the molecules have a preference to lie flat on the surface. In contrast, 5-FU was oriented at the steep angle of 58±5° on the Cu(111) surface after the deposition and the further annealing to 450K changed that angle to 63±5°.

We observed no evidence for scission of F from 5-FU following adsorption nor for annealing on either Au or Cu. Hence, these metal surfaces could be considered as suitable coating materials for the delivery of reactive drugs such as 5-FU, instead of silver surfaces, which are typically used in medical applications.

ACKNOWLEDGMENTS

We gratefully acknowledge the assistance of our colleagues at Elettra for providing good quality synchrotron light. CERIC-ERIC consortium and Czech Ministry of Education (LM2015057) are acknowledged for financial support.

REFERENCES

[1] L. Sanche, Radiat. Phys. and Chem. **128**, 36 (2016).
[2] J. B. Mitchell, A. Russo, J. A. Cook, K. L. Straus, and E. Glatstein, Int. J. Radiat. Biol. **56**(5), 827 (1989).
[3] R. W. Atcher, A. Russo, W. G. DeGraff, M. Moore, D. J. Grdina, and J. B. Mitchell, Radiat. Res. **117**(2), 351 (1989).
[4] T. S. Lawrence, M. A. Davis, J. Maybaum, P. L. Stetson, and W. D. Ensminger, Radiat. Res. **123**, 192 (1990).
[5] W. Zielenkiewicz and P. Szterner, J. Chem. Eng. Data **50**, 1139 (2005).
[6] P. V. Danenberg, H. Malli, and S. Swenson, Oncology **26**, 621 (1999).
[7] Y. He, C. Wu, and W. Kong, Chem. Phys. Lett. **391**, 38 (2004).
[8] W. Szybalski, Cancer Chemother. Rep. **58**, 539 (1974).
[9] N. Zhang, Y. Yin, S.-J. Xu, and W.-S. Chen, Molecules **13**, 1551 (2008).
[10] G. F. Paciotti, L. Myer, D. Weinreich, D. Goia, N. Pavel, R. E. McLaughlin, and L. Tamarkin, Drug Delivery **11**, 169 (2004).
[11] A. Lopez, Q. Chen, and N. V. Richardson, Surf. Interface Anal. **33**, 441 (2002).
[12] G. F. Paciotti, L. Myer, D. Weinreich, D. Goia, N. Pavel, R. E. McLaughlin, and L. Tamarkin, Drug Deliv **11**, 169 (2004).
[13] M. Irimia-Vladu, Chem. Soc. Rev. **43**, 588 (2014).
[14] E. F. Gomez, V. Venkatraman, J. G. Grote, and A. J. Steckl, Adv. Mater. **27**, 7552 (2015).
[15] M. Hoarau, C. Hureau, E. Gras, and P. Faller, Coord. Chem. Rev. **308**, 445 (2016).
[16] S. J. Sowerby, P. A. Stockwell, W. M. Heckl, and G. B. Petersen, Origins Life Evol. Biosphere **30**, 81 (2000).
[17] A. C. Papageorgiou, S. Fischer, J. Reichert, K. Diller, F. Blobner, F. Klappenberger, F. Allegretti, A. P. Seitsonenand, and J. V. Barth, ACS Nano **6**, 2477 (2012).
[18] I. D. Petsalakis and G. Theodorakopoulos, Isr. J. Chem. **45**, 127 (2005).
[19] H. L. Meyerheim and Th. Gloege, Chem. Phys. Lett. **326**, 45 (2000).
[20] Y. Cao, J. F. Deng, and G. Xu, Q. J. Chem. Phys. **112**, 4759 (2000).
[21] F. Cunha, E. Sá, and F. Nart, Surf. Sci. Lett. **480**, L383 (2001).
[22] H. B. de Aguiar, F. G. C. Cunha, F. C. Nart, and P. B. Miranda, J. Phys. Chem. C. **114**, 6663 (2010).
[23] F. Mazzola, T. T. Trinh, S. Cooil, E. R. Østli, K. Høydalsvik, E. T. B. Skjønsfjell, S. Kjelstrup, A. Preobrajenski, A. A. Cafolla, D. A. Evans, D. W. Breiby, and J. W. Wells, 2D Mater. **2**, 025004 (2015).
[24] D. V. Klyachko, M. A. Huels, and L. Sanche, Radiat. Res. **151**, 177 (1999).
[25] J. Peeling, F. E. Hruska, D. M. McKinnon, M. S. Chauhan, and N. S. McIntyre, Can. J. Chem. **56**, 2405 (1978).
[26] S. Irrera, G. Portalone, and N. H. De Leeuw, Surf. Sci. **614**, 20 (2013).
[27] F. Nazari and N. Ansari, Inter. J. of Quantum Chem. **112**, 2287 (2012).
[28] H. K. Risinggård, S. Cooil, F. Mazzola, D. Hu, M. Kjærvik, E. R. Østli, N. Patil, A. Preobrajenski, D. A. Evans, D. W. Breiby, T. T. Trinh, and J. W. Wells, App. Surf. Sci. **435**, 1213 (2018).
[29] O. Plekan, V. Feyer, N. Tsud, M. Vondráček, V. Cháb, V. Matolín, and K. C. Prince, Surf. Sci. **606**, 435 (2012).
[30] B. Hammer and J. K. Nørskov, Nature **376**, 238 (1995).
[31] R. Vašina, V. Kolařík, P. Doležel, M. Mynář, M. Vondráček, V. Cháb, J. Slezák, C. Comicioli, and K. C. Prince, Nucl. Instrum. Methods Phys. Res. A **467-468**, 561 (2001).
[32] D. Briggs, and M. P. Seah, *Practical Surface Analysis*, 2nd ed., John Wiley & Sons Ltd., 1990, Vol. 1, Auger and X-ray Photoelectron Spectroscopy.
[33] http://www.chemspider.com.
[34] V. Feyer, O. Plekan, R. Richter, M. Coreno, M. de Simone, K. C. Prince, A. B. Trofimov, I. L. Zaytseva, and J. Schirmer, J. Phys. Chem. A **114**, 10270 (2010).
[35] A. Haug, S. Schweizer, F. Latteyer, M. B. Casu, H. Peisert, C. Ochsenfeld, and T. Chasse, Chem. Phys. Chem. **9**, 740 (2008).
[36] O. Plekan, V. Feyer, A. Cassidy, V. Lyamayev, N. Tsud, S. Ptasinska, S. Reiff, R. G. Acres, and K. C. Prince, Phys. Chem. Chem. Phys. **17**, 15181 (2015).
[37] Th. Dretschkow and Th. Wandlowski, Electrochim. Acta **43**, 2991 (1998).
[38] W.-H. Li, W. Haiss, S. Floate, and R. J. Nichols, Langmuir **15**, 4875 (1999).
[39] F. Blobner, P. N. Abufager, R. Han, J. Bauer, D. A. Duncan, R. J. Maurer, K. Reuter, P. Feulner, and F. Allegretti, J. Phys. Chem. C. **119**, 15455 (2015).
[40] D. A. Duncan, W. Unterberger, D. Kreikemeyer-Lorenzo, and D. P. Woodruff, J. Chem. Phys. **135**, 014704 (2011).
[41] D. A. Duncan, J. H. K. Pfisterer, P. S. Deimel, R. G. Acres, M. Fritton, P. Feulner, J. V. Barth, and F. Allegretti, Phys. Chem. Chem. Phys. **18**, 20433 (2016).
[42] J. Stöhr, *NEXAFS Spectroscopy* (Springer-Verlag, Berlin, 1992).
[43] K. Fujii, K. Akamatsu, and A. Yokoya, J. Phys. Chem. B **108**, 8031 (2004).
[44] M. Furukawa, H. Fujisawa, S. Katano, H. Ogasawara, Y. Kim, T. Komeda, A. Nilsson, and M. Kawai, Surf. Sci. **532-535**, 261 (2003).
[45] F. Allegretti, M. Polcik, and D. P. Woodruff, Surf. Sci. **601**, 3611 (2007).